

Browse ▾

My Settings ▾

Get Help ▾

Subscribe

All ▾

Enter keywords or phrases (Note: Searches metadata only by default. A search for 'smart grid' = 'smart AND grid')



Search within Publication

Advanced Search

Other Search Options ▾

Browse Conferences > Progress in Electromagnetic Re... > 2018 Progress in Electromagnet... ?

Progress in Electromagnetic Research Symposium (PIERS)

Copy Persistent Link

Browse Title List

Sign up for Conference Alerts

Proceedings

All Proceedings

Popular

2018 Progress in Electromagnetics Research Symposium (PIERS-Toyama)

DOI: 10.23919/PIERS-Toyama43567.2018

Search within results



Per Page: 25 ▾

Export ▾

Email Selected Results ▾

Showing 1-25 of 472

Refine

Author ▾

Affiliation ▾

Select All on Page

Sort By: Sequence ▾

2018 Progress In Electromagnetics Research Symposium (PIERS | Toyama)

Publication Year: 2018, Page(s): 1 - 1

Abstract (158 Kb)



2018 Progress In Electromagnetics Research Symposium (PIERS | Toyama)

Publication Year: 2018 Page(s): 1 - 1



Need Full-Text

access to IEEE Xplore for your organization

Feedback

2018 Progress In Electromagnetics Research Symposium (PIERS — Toyama)

Copyright and Reprint Permission

© 2018 The Institute of Electronics, Information and Communication Engineer (IEICE). Personal use of this material is permitted. However, permission to reprint/republish this material for advertising or promotional purposes or for creating new collective works for resale or redistribution to servers or lists, or to reuse any copyrighted component of this work in other works must be obtained from the IEICE. As copyright holder for the PIERS 2018 Toyama Proceedings (abstracts and full-length papers), the IEICE grants the IEEE the nonexclusive, irrevocable, royalty-free worldwide rights to publish, sell, and distribute the copyrighted work for the Conference named above and any content derived from the copyrighted work in any format or media without restriction.

IEEE Catalog Number: CFP18C18-ART
ISBN: 978-4-88552-315-1 C3855

THE ELECTROMAGNETICS ACADEMY

The Progress in Electromagnetics Research Symposium (PIERS) is sponsored by The Electromagnetics Academy.

The Electromagnetics Academy is devoted to academic excellence and the advancement of research and relevant applications of the electromagnetic theory and to promoting educational objectives of the electromagnetics profession. PIERS provides an international forum for reporting progress and advances in the modern development of electromagnetic theory and its new and exciting applications.

Founded by the late Professor Jin Au Kong (1942–2008) of MIT in 1989, The Electromagnetics Academy is a non-profit organization registered in USA.

PIERS Founding Chair:

Jin Au Kong, MIT, USA

President of The Electromagnetics Academy:

Professor Leung Tsang, University of Michigan, USA

JOURNAL: PROGRESS IN ELECTROMAGNETICS RESEARCH

Progress In Electromagnetics Research (PIER) publishes peer-reviewed original and comprehensive articles on all aspects of electromagnetic theory and applications. This is an open access, on-line journal PIER (E-ISSN 1559-8985). It has been first published as a monograph series on Electromagnetic Waves (ISSN 1070-4698) in 1989. It is freely available to all readers via the Internet.

PIER is a non-profit organization.

WWW.JPIER.ORG

Contact Email: work@jpier.org

Founding Editor in Chief:

Jin Au Kong, MIT, USA

Editors in Chief:

Professor Weng Cho Chew, University of Illinois at Urbana-Champaign, USA

Professor Sailing He, Royal Institute of Technology, SWEDEN; JORCEP, Zhejiang University, CHINA

Progress In Electromagnetics Research Symposium
August 1–4, 2018
Toyama, JAPAN

PIERS 2018 TOYAMA ORGANIZATION

PIERS Chair

Leung Tsang, University of Michigan

PIERS 2018 Toyama General Chair

Kazuya Kobayashi, Chuo University

PIERS 2018 Toyama General Co-chairs

Weng Cho Chew, Purdue University

Sailing He, Royal Institute of Technology; JORCEP, Zhejiang University

Tsuneki Yamasaki, Nihon University

**PIERS 2018 Toyama Technical Program Committee Chair
and Co-Chairs**

Kazuya Kobayashi, Chuo University (Chair)

Ivan Andronov, St. Petersburg State University (Co-Chair)

Iam-Choon Khoo, The Pennsylvania State University (Co-Chair)

Qing Huo Liu, Duke University (Co-Chair)

Tadao Nagatsuma, Osaka University (Co-Chair)

Yoichi Okuno, South China Normal University; Kumamoto University (Co-Chair)

Motoyuki Sato, Tohoku University (Co-Chair)

Yury Shestopalov, University of Gävle (Co-Chair)

Ari Sihvola, Aalto University (Co-Chair)

Meisong Tong, Tongji University (Co-Chair)

Jan Vrba, Czech Technical University in Prague (Co-Chair)

Contents

Measurement and Modeling of Multi-frequency Microwave Emission of Soil Freezing and Thawing Processes	31
Z-R Relationships for Weather Radar in Indonesia from the Particle Size and Velocity (Parsivel) Optical Disdrometer	37
Imaging Plasma Inhomogeneities Using Spatial Wave Field Processing with DWFT Approximation ...	42
Optimal Cavities to Enhance Free-space Matching in Solar Cells	48
Parabolic Equation of Diffraction Theory: Why It Works Better than Expected?	53
Dipole Field Diffraction by a Strongly Elongated Spheroid in High-frequency Approximation	59
Diffraction of TM Polarized EM Waves by a Nonlinear Inhomogeneous Dielectric Cylinder	66
Measurement of the Diffraction Coefficient of a Trihedral Cone with Homogeneous Neumann Boundary Conditions	71
Heterogeneously Integrated Optoelectronic Devices for Implantable Neural Interfaces	78
A High-speed Pipelined ADC Based on Open-loop Amplification	82
A Chip of Pulse-laser-assisted Dual-beam Fiber-optic Trap	86
Rotation of a Trapped Microsphere in a Misaligned Dual-beam Optical Tweezer	92
Linear Cellularization Enabling Millimeter-wave Train Radio Communication Systems in 5G Era	99
Improvement in Accuracy of Breakpoint Distance Model for Path Loss Prediction	107
Effects of Storm Attenuation over Satellite Links in Sub-tropical Africa	115
A Comparative Study of Dual-slope Path Loss Model in Various Indoor Environments at 14 to 22 GHz	121
An Empirical Approach to Omnidirectional Path Loss and Line-of-sight Probability Models at 18 GHz for 5G Networks	129
The Second Order Moment Equation of Crossly Polarized EM-waves Due to Depolarization in Propagation through Continuous Isotropic Random Medium	137
Guided-mode Resonance in Waveguide Cavity	144
Microwave Interstitial Applicator Array for Treatment of Pancreatic Cancer	150
Microwaves in Medical Diagnostics and Treatment	155
Numerical Study of Stroke Detection Using UWB Radar	160
Prediction of Cement-based Materials' Water Content with the Use of Electromagnetic Homogenisation Schemes	164
Radar Bistatic Configuration for Soil Moisture Estimation at L-band Using Global Sensitivity Analysis Method	169
Two-slab High Sensitivity Technique for Measurement of Permittivity of a Dielectric Slab in a Rectangular Waveguide	176
Shape Measurement Based on Combined Reduced Phase Dual-directional Illumination Digital Holography and Speckle Displacements	184
A- Φ Formulation Time Domain Integral Equations Free from Interior Resonances	190
MOD Based Discontinuous Galerkin PMCHW Method for Simulating Transient Scattering Characteristics of Dielectric Objects	197

Fast Solution of Volume Integral Equations Based on Meshless Discretization	203
Analyzing Phased Arrays with Basis Functions Associated with Characteristic Modes	208
FDTD Analysis of Radiation and Reflection of Electromagnetic Fields in Finite Length Microstrip Lines with Terminal Cross-section	213
Uncertainties in EMC — Calibration and Testing	220
3D Holographic Display with Enlarged Field of View Based on Binary Optical Elements	227
Hydrophone Based on a Fiber Bragg Grating	233
Exploration of Optical Amplifiers Based on Erbium (Er^{3+}) and Ytterbium (Yb^{3+}) Doped Fiber Segments and Its Emerging Applications	237
Deep Learning for Interference Cancellation in Non-orthogonal Signal Based Optical Communication Systems	241
On-chip Detection from Directly Modulated Quantum Dot Microring Lasers on Si	249
Silicon-based Polarization Analyzer by Polarization-frequency Mapping	254
Optoelectronic Frequency Conversion Employing an Electro-absorption Modulated Laser for a Cube Satellite Earth Station	257
High SHF Band RF Signal Relay Employing Radio over Multi-mode Fibers	262
Modelling Defects on Junction between Coaxial Cables in View of Fault Diagnostic	266
Surface Electromagnetic Waves Propagation Guided by Dissipative Dielectric Material Sandwich between Two Periodic Multilayered Isotropic Materials in Prism Coupled Configuration	274
Modified Wang Shaped Ultra-wideband (UWB) Fractal Patch Antenna for Millimetre-wave Applications	280
Combined Electric and Magnetic Field Tuning of the Impedance of Lanthanum Strontium Manganite Thin Film Interdigital Electrode Devices	285
Magnetization State Determination Using Deep Learning	291
Ultra-broadband Tungsten Absorber	297
A Refined VR Based Video Indirect Ophthalmoscope	301
Fundamental Study for Optical Transillumination Imaging of Arteriovenous Fistula — System Integration into Practical Compact Device for Bedside Application	308
Monitoring of Nanopowder Combustion Ignited by Laser Radiation	311
Effect of Microwave Radiation on the Thermal Properties of the Electroexplosive Copper Nanopowder	317
Application of Laser-speckle Correlation Method for Blood Coagulation Estimation	320
The Development of a High Sensitive Micro Size Magnetic Sensor Named as GSR Sensor Excited by GHz Pulse Current	324
Engineering of GMI Effect of Fe-rich Microwires by Stress Annealing	332
Optimization of GMI Effect and Magnetic Properties of Co-rich Microwires by Joule Heating	338
Numerical Estimation Based on Ray Tracing for Automotive Radar Beam Through Curved Dielectric Slab	344
Electric Field Strength in Layered Materials with Varied Parameters	347
On the Evaluation of Sources in Highly Accurate Time Domain Simulations on the Basis of Faber Polynomials	352
Extension of the Parabolic Equation Method in the Time Domain	357
A Fast Algorithm for Electromagnetic Scattering from One-dimensional Dielectric Rough Surface	362
SRCNN-based Enhanced Imaging for Low Frequency Radar	366
An Improved Algorithm for Enhancing Fingerprint Image Quality	371
A High-speed Data Acquisition and Preprocessing Method for Wirelessly Supervising Train Braking System	376

Characteristic Parameter Estimation of Chipless RFID Signals Based on USRP	381
NDF and On-axis Resolution of an Axicon in Near Zone: Numerical Experiments	386
On the Number of Independent Equations in Phase Retrieval Problem: Numerical Results in Circular Case	392
Programmable Pulse Processor Using Cascaded Microrings on Silicon Photonic Circuits	396
WT-based Data-length-variation Technique for Fast Heart Rate Detection	399
Transmission Line Analogy for Wave Propagation in Graphene-based Structures	405
Emulating Tunneling with Elastic Vibrating Beams	410
Design of RFID Tag Antenna Based on the Cole-Cole Model of Human Abdomen	414
Characteristics of 340 GHz Slow Wave Structure for Staggered Double-vane Traveling Wave Tube	420
Design and Modeling of Tunable Band-stop Filter Using Evanescent Mode Resonators	424
An Example of Notch Filter Design Spec for the IM Noise Signal Cancellation in 800 MHz CDMA Frequency Band	428
Influence of Tropospheric Ducts on Radio Propagation over Sea Surface	432
Mode Absorption Filters Based on Graphene-on-silicon Waveguides	437
Optical Force for Particle Trapping in a Nanobeam Photonic Crystal Cavity	440
Analysis of Interferogram Phase Noise by Bi-static Data Sets of TerraSAR-X	444
Modified Helical Coils Structure for Uniform Magnetic Flux Density	449
A Low-profile Antenna Design for LTE/WWAN Smartphone Application	454
Eutrophication Analysis of Water Reservoirs by Remote Sensing and Neural Networks	458
Filtered Back Projection and Simultaneous Algebraic Reconstruction Technique for Image Formation on Square-shaped Physical Phantom Aimed at Microwave Imaging Applications	464
Estimation of the Energy Characteristics of a Multi-position Radar System for the Control of Small-sized Space Debris for Various Orbital Zones	470
Estimation of the Resolution of a Multi-position Radar for the Control of Small-sized Space Debris Objects That Are Not Resolved by Angular Coordinates	476
Efficient Electromagnetic Scattering Analysis for Multi-scale Problems Using Green's Functions of Arbitrary Scatterers	482
Plasmonic Properties of Electrolytes beyond Classical Nanophotonics — A Two-fluid, Hydrodynamic Approach to Nonlocal Soft Plasmonics	490
Modeling the Magnetic Field Radiated from a Ferrite Rod Antenna for Mining Proximity Detection Systems	496
A Novel Approach to Microfabrication of Planar Microstrip Meander-line Slow Wave Structures for Millimeter-Band TWT	506
Radiation Pattern Inspection of the FMCW Signal Using Asynchronous Electro-optic Measurement System	510
Novel Measurement Set-ups of FTB Stress Propagation in an IC	513
Speed of Light in Vacuum in the Case of a Lumped Electric Circuit	520
Numerical Models of a Multilayered Graphene Structure	527
Algorithms to Detect and Localize the Source of a Wideband Pulse Signal	533
A Numerical Analysis of a Periodic Resonant Structure at THz Frequencies	537
Vision-based and Differential Global Positioning System to Ensure Precise Autonomous Landing of UAVs	542
High Frequency Scattering from Conducting Rectangular Cylinder via Surface Equivalence Theorem ..	547
<i>H</i> -polarized Plane Wave Diffraction by Thick Conducting Slits	553

An Enhanced Model for the Analysis of Non-uniform Multiconductor Transmission Lines Based on Scattering Theory	559
Spatial Prediction of Electromagnetic Fields Using Few Measurements	565
Coupling of Differential and Common Modes of Two-line Circuits in the Multi-conductor Transmission-line Theory Including Radiation	570
Orbital Angular Momentum Generation Using Composite Quasi-continuous Metasurfaces with Perfect Efficiency	575
Giant Nonlinear Response of Subwavelength Dielectric Resonators Enhanced by Bound States in the Continuum	580
Metasurfaces for Improvement Magnetic Resonance Imaging Characteristics: Novel Designs and In Vivo Studies	585
Characterization of Terahertz Plasmonic Structures Based on Metallic Wire Woven Meshes	588
Helicity-induced Multifunctional Devices Based on Hybrid Metasurfaces	592
Integrated Circuits Using Photonic-crystal Slab Waveguides and Resonant Tunneling Diodes for Terahertz Communication	599
Improved Detection Strategies for Nonlinear Frequency-division Multiplexing	606
Open Area Concealed Weapon Detection Sensor System Development	611
Design and Analysis of Inductive Reluctance Position Sensor	621
Wireless Energy Harvesting in RFID Applications at 5.8 GHz ISM Band, a System Analysis	627
A Novel Microwave Applicator for Sandy Soil Disinfection	636
Study of Simultaneous Switching Noise in Two-dimensional Transport Theory including Radiation Effect	642
Effect of Absorbing Coating on Shielding Effectiveness of Electromagnetic Shielding Fabric	648
Optimal Design of Yagi Microstrip Antenna Based on Particle Swarm Optimization with Fitness Estimation	653
Analysis of Singular-point Generating Mechanisms Based on the Correlations among the Parameters in Coherency Matrix and Those in the Optimized Scattering-mechanism Vector in PolInSAR	661
Imaging Performance of Backward and Forward Bistatic SAR	669
Adaptive Subsurface Visualization System Using Phase Retrieval Method and Complex-valued Self-organizing Map	677
Influence Analysis of Uneven Surface on Landmine Detection Using Holographic Radar	683
A 3.5–8 GHz Analog Complex Cross-correlator for Interferometric Passive Millimeter-wave Security Imaging Systems	692
Shuffled Structure for 4.225 GHz Antireflective Plates: A Proposal Proven by Numerical Simulation ...	700
A Modified Method for Measuring the Faraday Rotation Angle	706
Data Augmentation Using Conditional GANs for Facial Emotion Recognition	710
An Efficient Face Recognition Algorithm Based on Deep Learning for Unmanned Supermarket	715
Efficient Data Record System for Radio Backend	719
Pre-processing VDIF Data in FPGA	723
A Novel Extraction Method for Melodic Features from MIDI Files Based on Probabilistic Graphical Models	729
Model Calculations for Hardware Correlator at SHAO	734
Waveguide BPF Composed of Dielectric Frequency Selective Structure with High Suppression of Spurious Mode	739
Design Optimization of RF-MEMS Based Multiband Reconfigurable Antenna Using Response Surface Methodology	743

Indoor Localization System Using Commensal Radar Principle	751
An Improved Successive-cancellation Decoding Algorithm for Polar Code Based on FPGA	756
Improved Electromagnetic Compatibility Design for Printed Circuit Board of Automobile Atmosphere Lamp	760
Next Approach of HEMS WPT	765
Numerical Study of Hyperthermia Applicator System for Tumor Treatment in Head and Neck Region	770
An Interference EMG Model of Selected Water Samples	775
Algorithms for Flying Object Detection	782
Formation of Ray Trajectories of HF Radiowaves in Midlatitude and Highlatitude Ionosphere during Halloween Storm 2003 According to Radiotomography Data	787
Multiple-bounce Modeling of High-rise Buildings with Airborne Tomography Array	791
The Study of Composite Scattering from the Target over a Randomly Rough Surface Using SAR/ISAR Imaging	797
Scattering Characteristics of Vortex Electromagnetic Waves for a Wedge	801
Application of the RK4IP Method for the Numerical Study of Noise-like Pulses in Supercontinuum Generation	805
Numerical Analysis of Chaotic Dynamics Produced in a Photonic Crystal Fibers	810
Classification and Properties of Modes in Bragg Fibers	814
Inverse Synthetic Aperture Ladar Imaging Algorithm for Space Maneuvering Target Using Synchrosqueezing Short-time Fourier Transform	819
Analysis of Spectrum Properties of Integrated Optical Chips Applied on IFOG	827
Semi Circular Printed Monopole Antenna with \cup Shaped Slot for UWB Applications	833
Design of 5 Way Wide Band Wilkinson Power Divider for 6 to 18 GHz Applications	838
Magneto-optical Properties of a Magnetic Fluid in the THz Frequency Range	843
Multiband Circularly Polarized Synthetic Aperture Radar (CP-SAR) Onboard Microsatellite Constellation	848
Comparison Design of X-band Microstrip Antenna for SAR Application	854
Gain Enhancement of C Band Linearly-polarized Microstrip Antenna with Square Parasitic Patch for Airborne LP-SAR Sensor	858
Dual-band Circularly-polarized Microstrip Antenna for Nano Satellite	864
3D Printed Wideband Circularly Polarized Pyramidal Horn Antenna	868
Unidirectional Radiation and Gain Enhancement of Circularly Polarized Printed Slot Antenna by Several Shapes of Reflector	872
An 8-channels FPGA-based Reconfigurable Chirp Generator for Multi-band Full Polarimetric Airborne/Spaceborne CP-SAR	876
An PC-based Airborne SAR Baseband System	882
Numerical Solution for Received Power Estimation in a Wave Propagation — A Case of Ground Based C-band SAR Test	889
Indoor Experiment of SAR Interferometry with 79 GHz MIMO Sensor	894
Single Post-event PolSAR Data Based Earthquake/Tsunami Damage Information Extraction in Urban Areas	899
Interferometry Synthetic Aperture Radar (InSAR) Application for Flood Area Detection Observed by Sentinel 1A	905
Multi-temporal Land Deformation Monitoring in V Shape Area Using Quasi-Persistent Scatterer (Q-PS) Interferometry Technique	910

Numerical Solution for Received Power Estimation in a Wave Propagation — A Case of Ground Based C-band SAR Test

M. Nasucha^{1,2}, J. T. S. Sumantyo¹, M. Y. Chua¹, C. E. Santosa¹, Y. Izumi³, and P. Razi¹

¹Center of Environmental Remote Sensing, Chiba University, Chiba 263-8522, Japan

²Department of Informatics & Computer Science, Universitas Pembangunan Jaya
Tangerang Selatan, Indonesia

³Graduate School of Environmental Studies, Tohoku University, Japan

Abstract— Despite the long history and wide application of computer simulation on wave propagation, it is found interesting that study on numerical solution to estimate the amount of received power at the receiving antenna is limited. While, in preparing a radio transmission system, including a SAR system, the estimation of received power is crucial. A good estimation on received power shall reduce the probability of an on-field failure. This article is mainly aimed to addresses several aspects in conceiving the solution to this issue. In particular, a ground-based C-band SAR test scenario using a 5.3 GHz carrier and our newly designed transmitting and receiving antennas has been taken as a case as the simulation model.

1. INTRODUCTION

Computer simulation on wave propagation has been studied widely for various purposes, including the ones reported in [1–6]. Nagatani et al. [1] reported study on the propagation of ultrasonic waves for medical imaging purpose. H. B. Lim et al. [2] and S. C. Hagness et al. [3] reported their study on the propagation of microwave for the medical imaging purpose too. V. Jokovic et al. [4] addressed study on the propagation of microwave for the purpose of material heating. M. Qakir, G. Qakir and L. Sevgi [5] discussed outcome of their study on wave propagation in a context of (future) device development, especially ones involving metamaterials.

Despite the varied properties of the waves in use and the varied purposes for which the studies have been carried out, these works had a similarity: the computer simulations on the wave propagation were done for a (very) short traveling range, i.e., a few λ s to tens of λ s. The reason for this trend to develop is that a computer simulation for wave propagation requires a huge computation resource especially for carrying out a large number of iterations. Research work on numerical simulation of wave propagation over a large area is still limited. This kind of research was reported in [6]. In this paper B. Dowd and R. E. Diaz simulated a radio wave propagation over an area of the ocean using Finite Difference Time Domain (FDTD) method.

Beside the fact that study on wave propagation over a large area is limited, it is interesting to find that most numerical computations on the wave propagation — mostly using Finite Difference Time Domain (FDTD) method, Method of Moment (MoM) and Finite Element Method (FEM)- have not focused on the estimation on the power density at the receiving point. While, estimating power density at the receiver point is a crucial requirement, as part of the power budget planning. A good estimation on the received power density should provide confidence to a researcher or engineer in obtaining best signals.

Take an example, the importance of power density estimation is found in Synthetic Aperture Radar (SAR) remote sensing practices. The SAR remote sensing itself is usually done using a satellite, an aircraft, or a ground vehicle. An example of the usage of a useful satellite SAR data for humanity is reported in [7].

This article is aimed to address our initial work in conceiving a numerical solution for estimating power density over space and time difference. A real case of ground-based SAR test conducted by our lab is taken as a model in order to show a more perceptible explanation.

2. PROBLEMS AND PROPOSED SOLVING METHOD

In this section the problem is addressed and elaborated, as well as our proposal on the method of solving it.

2.1. Problems

In a radio transmission system a power budget planning is required in order for the receiver to receive signals as desired. Harald. T. Friis is the first person worked on and published the relation between transmitted and received radio wave power in a radio transmitting system consisted of a transmitter and a receiver that are separated each other by a certain distance [8]. Following some elaboration, the Friis Formula then can be expressed as

$$Pr = \frac{Pt \cdot Gt \cdot Gr \cdot \lambda^2}{(4\pi d)^2} \quad (1)$$

where Pr is the received power at the receiving antenna (watt), Pt is the transmitted power at the transmitting antenna (watt), Gt is the transmitting antenna's gain, Gr is the receiving antenna's gain, d is the distance between the two antennas (m) and λ is the wavelength of the radio wave in use (m).

The above equation is fulfilling the requirement in estimating the received power at the receiving antenna that receives waves directly from the transmitting antenna. However, a problem occurs as in a SAR remote sensing double hopping happens, where the transmitted waves hit an object first then reflected towards the receiving antenna. This problem is visually explained by Figure 1. This problem requires a solving approach.

Secondly, in the context of dynamic computation, there is a discretization issue, that is, that there should be an approach to produce output values at any x - y position.

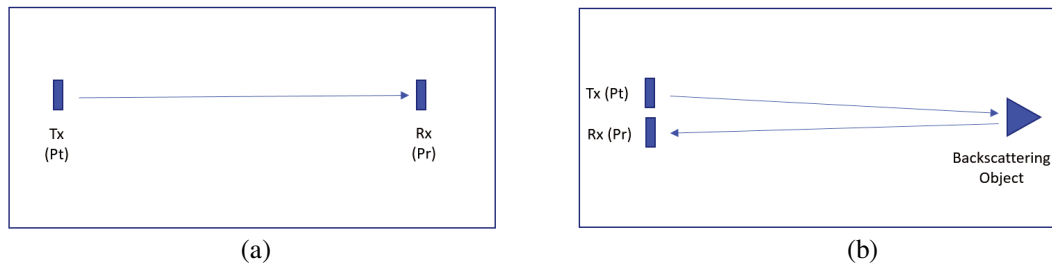


Figure 1: (a) shows a line-of sight radio wave transmission event where the Friis Formula directly applies, (b) explains the first problem (challenge) occurs in an event of SAR remote sensing; multihopping, where Friis Formula needs to be elaborated.

2.2. Proposed Solving Method and Algorithm

2.2.1. Solving the Multihopping Problem

We are proposing the solution method for the first problem as mentioned in sub-section 2.1 principally by dividing the transmission path into two legs, that are, leg1 the departing path (from Tx to object) and leg2 the returning path (from object to Rx). This method is then elaborated into the path splitting algorithm as depicted by Figure 2.

2.2.2. Solving the Discretization Problem

In general discretization is done at every computer simulation method, including ones that are addressed in [9–11]. In this particular challenge, the approach is to derive Equation (4) in a way so that Pr can be calculated dynamically, i.e., calculable for every space change (dx , dy) and time change (dt). Figure 3 visually explains the conception of the discretization applied in our study.

3. COMPUTATION MODEL

In our study the elaboration of the method is still improving. However, each conception progress was realized into our MATLAB coding. In this regard, a real case of Ground Based C-band SAR Test has been taken as the computation model.

3.1. Assigning Values to the Wave Propagation Constants and Variables

Values are assigned to the wave propagation variables in accordance to our Ground Based C-band SAR Test that has been carried out on the June 15, 2017. These values are as follows: $co = 2.9979e8$ m/s, $f = 5.3$ GHz, $\epsilon_o = 8.8542e - 12$ F/m, $\mu_o = 1.2566e - 6$ H/m, transmitting power = 44 dBm (25 watt), transmitting antenna's gain = 23.42 dBi(219), receiving antenna's gain = 23.42 dBi(219), backscattering object's relative permittivity, $\epsilon_r = 10.8$, backscattering object's

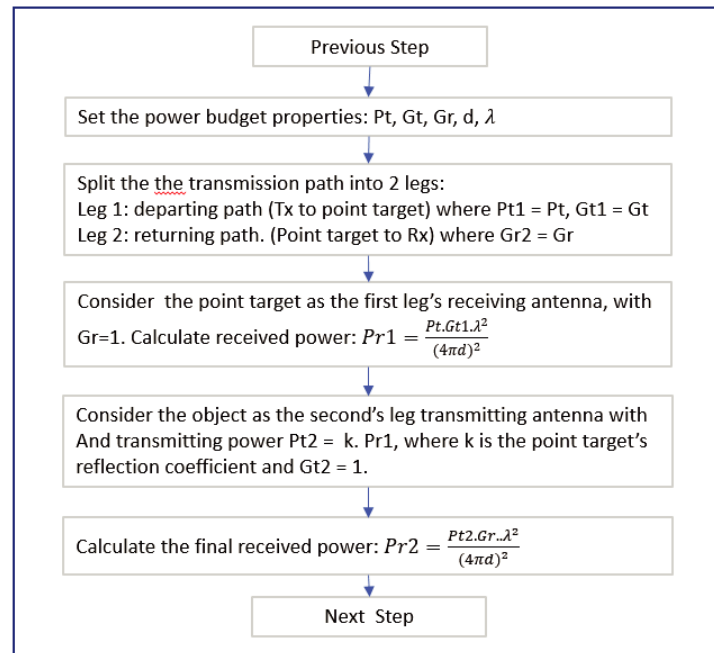


Figure 2: Proposed Path Splitting Algorithm, as a solution to the multihopping problem. The value of k shall be computed based on point target (object)'s material permittivity and surface roughness.

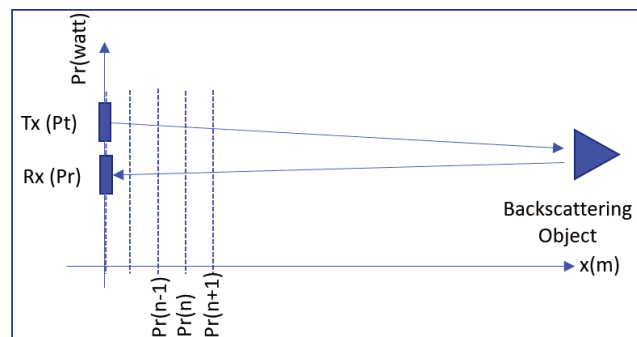


Figure 3: This explains our conception of the discretization. For simplicity here only one-dimension discretization of P_r is shown. When carrying out an FDTD computation, statically usage of Friis Formula is not applicable because $P_r(n)$ shall be computed based on $P_r(n-1)$, instead of $P(0)$ or the transmitting power (P_t).

relative permeability $\mu_r = 1$, receiver sensitivity = -85 dBm (3.16 pw). The assignment of these values into the computer program's variables and constants is depicted by Figure 4.

3.2. Confirming the Position of SAR Test Elements

In a ground-based SAR test, the position of the SAR device (Tx/Rx), the azimuth length, the range length and the position of the backscattering object (point target) relative to the Tx/Rx is also crucial. In the MATLAB program we visualized this position setting and it is here depicted in Figure 4. The visualization of correct position of each element provided confidence in proceeding with the computation.

4. PRELIMINARY RESULT AND DISCUSSION

While this study is still on-going, some preliminary results of are here presented. Figure 5 shows the simulation states at the first leg (propagation between the Tx antenna and the corner reflector) whereas Figure 6 shows the simulation states at the second leg (propagation between the corner reflector and the Rx antenna).

The simulation resulted in several reasonable data: from Figures 5 and 6 — even clearer from the video clip- it is seen that the value of P_r decreases with travel distance and travel time. It can

be seen from Figure 6(a) that at an early time step, at the distance of 26.8 m the wave power is 15.23 dBm. It is interesting to find in Figure 7(b), the value of the final state of the simulation: the net power received by the receiving antenna is -2.13 dBm. This indicates that the study has been able to show the right trend of the data. However, the accuracy of these numerical values is subject to further assessment.



Figure 4: Visualization of the SAR test elements within the program. The vertical line is the azimuth line (Y -axis), the horizontal line is the range line (X -axis), the two white bars in the left side are the transmitting antenna and the receiving antenna, the white bar in the right side is the corner reflector (point target). Distance between antenna and the corner reflector is 100 m.

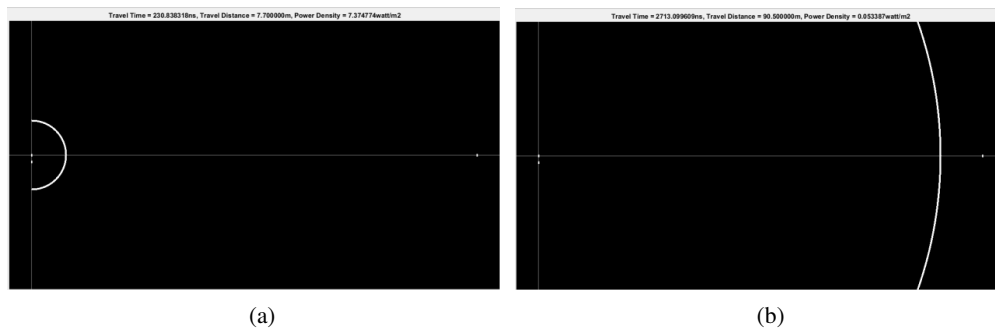


Figure 5: This figure shows states of the simulation at two different time steps of the first leg: (a) is at an early time step, that is, a while after the wave departed from the Tx antenna, (b) is at a late time step, that is, when the wave is approaching the corner reflector.

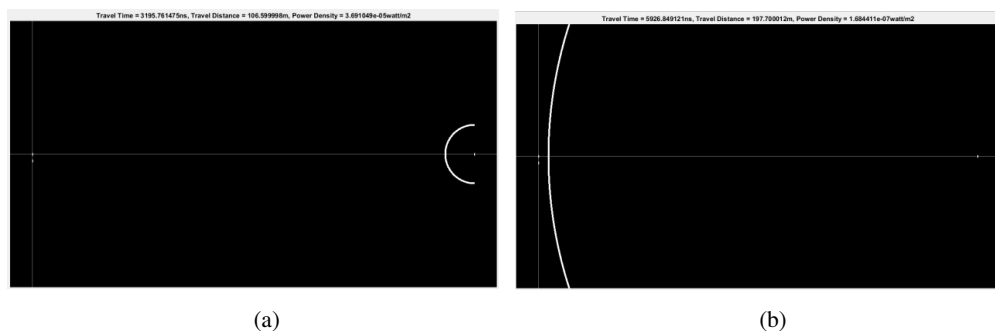


Figure 6: This figure shows states of the simulation at two different time steps of the second leg: (a) is at an early time step, that is, a short time after reflection by the corner reflector, (b) is at a the final time step, that is, when the wave is about to reach the receiving antenna.

5. CONCLUSION

Out of this study, it can be recognized that (i) in a computer simulation on wave propagation dynamic calculation of wave power is possible, (ii) the dynamic calculation of the wave power

can be done using the method and algorithm proposed in this paper, (iii) by doing so, estimating the received power at the receiver antenna of a ground-based SAR is possible. However, it is to be noticed that this study is still on-going, thus will probably result in further updates and correction(s) in the future.

ACKNOWLEDGMENT

We would like to convey our gratitude to Mitsubishi Corporation International Student Scholarship for their funding support to the study, as well as the Ministry of Research, Technology and Higher Education of the Republic of Indonesia (Kemenristekdikti) for their support to the research.

REFERENCES

1. Nagatani, Y., et al., “Numerical and experimental study on the wave attenuation in bone-FDTD simulation of ultrasound propagation in cancellous bone,” *Ultrasonics*, Vol. 48, 607–612, 2008.
2. Lim, H. B., et al., “Confocal microwave imaging for breast cancer detection: Delay-multiply-and-sum image reconstruction algorithm,” *IEEE Transactions on Biomedical Engineering*, Vol. 55, No. 6, 1697, June 2008.
3. Hagness, S. C., et al., “Two-dimensional FDTD analysis of a pulsed microwave confocal system for breast cancer detection: Fixed-focus and antenna-array sensors,” *IEEE Transactions on Biomedical Engineering*, Vol. 45, No. 12, December 1998
4. Jokovic, V., et al., “FDTD simulation of microwave heating of variable feed,” *Minerals Engineering*, Vol. 59, 12–16, 2014.
5. Qakir, M., G. Qakir, and L. Sevgi, “A two-dimensional FDTD-based virtual visualization tool for metamaterial-wave interaction,” *IEEE Antennas and Propagation Magazine*, Vol. 50, No. 3, 166–175, June 2008
6. Dowd, B. and R. E. Diaz, “FDTD simulation of very large domains applied to radar propagation over the ocean,” *IEEE International Symposium on Antennas and Propagation & USNC/URSI National Radio Science Meeting*, San Diego, 2017.
7. Razi, P., et al., “3D land mapping and land deformation monitoring using persistent scatterer interferometry (PSI) ALOS PALSAR: Validated by geodetic GPS and UAV,” *IEEE Access*, Vol. 6, 12395–12404, February 2018.
8. Friis, H. T., “A note on a simple transmission formula,” *Proc. IRE*, 254–256, 1946.
9. Inan, U. S. and R. A. Marshall, *Numerical Electromagnetics: The FDTD Method*, Cambridge University Press, New York, 2011.
10. Yu, W., et al., *Electromagnetic Simulation Techniques Based on the FDTD Method*, John Wiley & Sons, New Jersey, 2009.
11. Taflove, A. and S. C. Hagness, *Computational Electrodynamics: The Finite-Difference Time-Domain Method*, 3rd Edition, Artech House, Norwood, MA, 2005.



公益財団法人

電気通信普及財団

The Telecommunications Advancement Foundation



公益財団法人

Toyama Convention Bureau

富山コンベンションビューロー



公益財団法人 村田学術振興財団

The Murata Science Foundation

